ARCHITECTURAL RESEARCH, Vol. 10, No. 2(December 2008), pp.27-35

Confining Effect of Mortar-filled Steel Pipe Splice

Hyong-Kee Kim
Department of Architectural Engineering, Kangwon National University, Samcheok, Korea

Abstract

Because of several advantages of mortar-filled sleeve splice in reinforced concrete buildings, this method is being applied increasingly at construction sites and various methods of the splice have been developed in Korea and other countries. In order to apply this system in the field, studies on mortar-filled sleeve splice have been mainly experimental research focused on overall structural performance. However, for understanding the structural characteristics of this splice more accurately, we need to study the confining effect of sleeve, which is known to affect bond strength between filling mortar and reinforcing bar, the most important structural elements of the bar splice.

Thus, in order to examine the confinement effect of mortar-filled steel pipe sleeve splice, the present study prepared actual-size specimens of steel pipe sleeve splice, and conducted a loading. Using the test results, we analyzed how the confining effect of steel pipe sleeve affects the bond strength of this splice and obtained data for developing more reasonable methods of designing the splice of reinforcement.

Keywords : Confining Effect, Mortar-filled Steel Pipe Splice, Bond Strength

1. INTRODUCTION

Splice of reinforcement in reinforced concrete structure can be largely divided into lap splice, welded splice and mechanical splice. Among them, mortar-filled sleeve splice, which is a type of mechanical splice, is being used very effectively for the reinforcing bar splice because it is highly applicable to commonly used large-diameter bars and highly workable in the field, and enables stable quality and the minimization of work force. Because of these advantages of the splice, various reinforcement splice methods have been developed in Korea and other countries. In order to apply this system in the field, studies on mortar-filled sleeve splice have been mainly experimental research focused on its overall structural performance (Ase et al., 1996; Lee et al., 1997; Kim, 1998; Lee and Kim, 2007; Kim, 2008). However, for understanding the structural characteristics of this splice more accurately, we need to study the confining effect of sleeve, which is known to affect bond strength between filling mortar and reinforcing bar, the most important structural elements of the bar splice.

Generally in reinforced concrete structures, confining pressure on concrete is known to increase bond strength between bars and concrete. The confinement effect of reinforced concrete members has been examined by several researchers through experimental and analytic research centering on members receiving axial force or flexure. However, not many studies have been made on how the effect of confinement works on the bond strength of single reinforcing bar elements as in mortar-filled sleeve splice. Among them, Untrauer and Henry (1965) made 37 reinforced concrete specimens and conducted a pull-out test by applying normal pressure to them, and reported that bond strength between deformed bars and concrete is linearly proportional to the square root of normal pressure. In addition, for examining the confining effect of steel pipe on bond strength between bar and mortar in mortar-filled steel pipe splice, Einea et al. (1995) prepared specimens of steel pipe splice for D16 and D19 reinforcing bars and conducted a monotonic loading. They also computed confining pressure working on the splice using data from strain gauges attached to the surface of the sleeve. However, their computation of confining pressure on the sleeve was somewhat inaccurate because it did not consider Poisson's effect occurring in the sleeve. On the other hand, Ahn et al. (2003) examined the effect of confinement in mortar-filled cast sleeve splice by preparing specimens of sleeve splice for small-diameter reinforcing bars (D19, D25) and conducting a monotonic loading. They also computed confining pressure working on mortar-filled cast sleeve splice, and examined how the confinement action of the sleeve affects the bond strength of the splice.

As presented above, previous researches on the confining effect of sleeve splice of reinforcement were mostly limited to monotonic loading experiments using specimens for reinforcing bars of small diameter below D25. Thus, for more accurate evaluation of the confinement effect of sleeve in mortar-filled sleeve splice, we need experimental research on the confining effect of various variables.

Thus, the present study purposed to provide basic engineering data for establishing more reasonable methods of designing mortar-filled sleeve splice by conducting an experiment with steel pipe sleeve splice developed recently for SD500 reinforcing bars (Lee and Kim, 2007; Kim, 2008) using variables such as the development length of reinforcement, the bar size and loading method, and analyzing the confining effect of mortar-filled steel pipe sleeve.

2. EXPERIMENT

2.1 Specimen planning and preparation

Major experimental variables considered in this study are as follows.

1) The development length of reinforcing bars in sleeve (L_d=7.5d, L_d=5d, where d is the nominal diameter of the bars)
2) The compressive strength of filling mortar (28-day specified compressive strength is 75MPa, 95MPa)
3) The bar size (D25, D32)
4) Loading method (monotonic loading, cyclic loading)

Based on these experimental variables, we prepared 7 actual-size specimens as in Table 1, and attached two-direction strain gauges, which can measure axial and tangential strain in sleeve, on the surface of the steel pipe sleeve of each specimen. Figure 1 shows details of the specimens. Details of steel pipe sleeve for D32 bar are shown in Figure 2. The steel pipe sleeve was manufactured as shown in Figure 2, using the steel molds made exclusively for the fabrication of sleeve. In addition, Figure 3 shows the locations of strain gauges attached on the surface of sleeve for the splice of D32 reinforcement. Here, the interval between the strain gauges was set according to the interval of lugs on the reinforcing bars embedded in the sleeve.

Table 1. List of specimens

No.	Specimens name	Experimental variable			
		Bar size	L_d *1 (d)	Compressive strength of mortar (MPa)	Load method*2
1	27B'1NM-1	D25	7.5	75	M
2	37B2HM-1	D32	7.5	95	M
3	37B2NM-1	D32	7.5	75	M
4	35B2NM-1	D32	5.0	75	M
5	37B2NC-1	D32	7.5	75	C
6	37B2HC-1	D32	7.5	95	C
7	35B2NC-1	D32	5.0	75	C

(Note) *1 : Development length of reinforcing bar
*2 : M=Monotonic loading, C=Cyclic loading

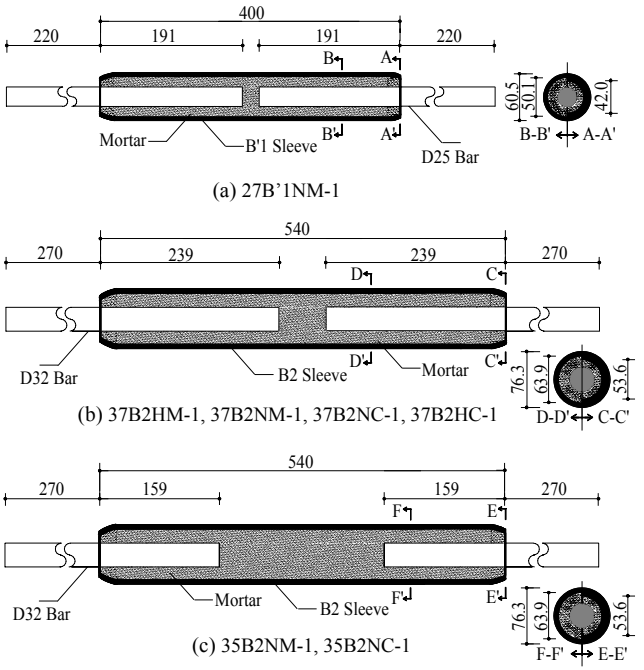

(a) 27B'1NM-1

(b) 37B2HM-1, 37B2NM-1, 37B2NC-1, 37B2HC-1

(c) 35B2NM-1, 35B2NC-1

Figure 1. Details of specimens

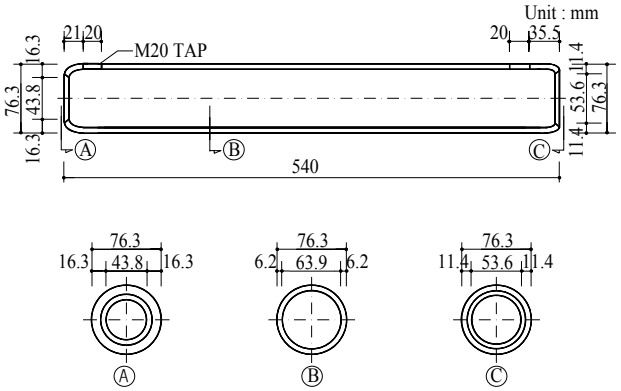

Figure 2. Details of sleeve for D32 bar (Kim, 2008)

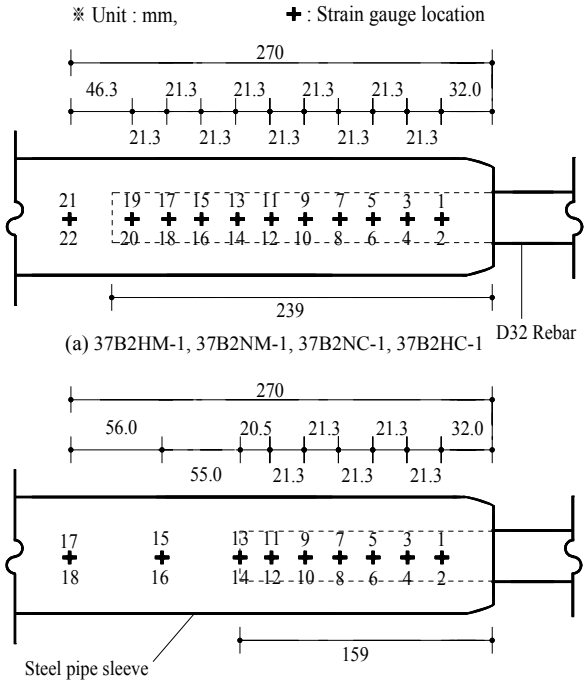

(a) 37B2HM-1, 37B2NM-1, 37B2NC-1, 37B2HC-1

(b) 35B2NM-1, 35B2NC-1

Figure 3. The location of strain gauges on the sleeve surface of specimens for D32 bar

For high-strength mortar filling of the specimens, we set the sleeve upright and filled it with mortar through the inlet on the bottom of the sleeve using a mortar filling pump so that the mortar filling was done in the same condition as actual construction sites. The mixture ratio of water to mortar was 15%, and mixing time was around 2 minutes. On the other hand, after mortar filling and curing were completed, strain gauges were attached to the locations on the surface of sleeve as in Figure 3.

2.2 Mechanical characteristics of materials

This test used reinforcing bar SD500. Table 2 shows the test results of the tensile strength.

This test used two kinds of steel pipe sleeve. The sleeve for D32 bars was a steel pipe 76.3 mm in external diameter and 6.2mm in thickness, which improved the mechanical properties by adjusting the chemical elements of STK 490.

Table 2. Mechanical properties of reinforcing bar

Bar size	Yield strength (MPa)	Tensile strength (MPa)	Elongation ratio (%)
D25	575	689	19.6
D32	556	696	21.2

Table 3. Mechanical properties of steel pipe material

Steel pipe type			Yield strength (MPa)	Tensile strength (MPa)	Elongation ratio (%)
Bar size	d_e*1/ t*2 (mm)	With/out heat treatment			
D25	60.5/ 5.2	with	306	525	27.5
D32	76.3/ 6.2	without	478	567	30.0

(Note) *1 : External diameter of steel pipe
*2 : Thickness of steel pipe

Table 4. Quality standard of mortar (Kim, 2008)

Items \ Mortar kind		N mortar*1	H mortar*2
Time of efflux <J14 flow cone> (Seconds)		10±5	20±5
Setting time (Hours : Minutes)	Initial set	3:30	3:30
	Final set	6:30	6:30
Compressive strength (MPa)	3 days	45	65
	7 days	55	80
	28 days	75	95
Water-cement ratio (%)		15	15

(Note) *1 : Existing non-shrinkage mortar
*2 : Newly developed non-shrinkage mortar

Table 5. Compressive strength of mortar

Specimen / Mortar type	Monotonic loading specimen*1 (MPa)	Cyclic loading specimen*2 (MPa)
N mortar	82.3	83.8
H mortar	83.0	83.9

(Note) *1 : 27B'1NM-1, 37B2HM-1, 37B2NM-1, 35B2NM-1
*2 : 37B2NC-1, 37B2HC-1, 35B2NC-1

And the sleeve for D25 bars was a steel pipe 60.5mm in external diameter and 5.2mm in thickness for STPG 370 pressure piping, which was heat-treated to improve mechanical properties. Table 3 shows the test results for tensile strength of the two types of steel pipe material above.

In this test, two kinds of high-strength non-shrinkage filling mortar were used. One is existing product, and the other a newly developed one, which has higher compressive strength than existing ones. The quality standards of the two types of filling mortar are shown in Table 4. Contrary to our expectation, however, in the test results of compressive strength, the two kinds of mortar did not show a difference in compressive strength as in Table 5. The compression test was conducted according to ASTM C 109 (1995) using 5cm×5cm×5cm cubic specimens.

2.3 Loading and measuring methods

In this test, monotonic loading was performed using a 2,000kN Universal Testing Machine, and cyclic loading was performed using Instron 4495 Universal Testing System(see Figure 4), which can load up to 1,200kN and apply tensile force and compressive force continuously to specimens. The displacement of sleeve splice was measured using two Linear variable displacement transducers (LVDTs) installed between the measuring devices attached to the bars 20mm apart from the top and bottom ends of the sleeve. In loading schedule, monotonic loading on the specimens was raised gradually until tensile strength became 95% of the specified yield strength (f_y) of the reinforcing bars of the specimens, and then after the load was removed, tensile force was again raised gradually until the specimens broke. On the other hand, cyclic loading within the scope of elasticity was applied 20 times repeatedly so that tensile stress 95% of the specified yield strength of the bars worked in the tension direction and compressive stress 50% of the specified yield strength of the bars worked in the compression direction. And then cyclic loading within the scope of plasticity was applied 4 times so that compressive stress 50% of the specified yield strength of the bars worked in the compression direction after loading up to two times higher than the yield strain of the specimens in the tension direction. In case loading was performed continuously up to 5 times higher than the yield strain of the specimens as well, load was applied in the same method and finally the specimens were broken by tensile force.

In each stage of this test, the following items were measured and recorded.

1) Load applied to the specimen
2) Relative displacement between the displacement measuring points of the specimens
3) Axial and tangential strain on the surface of sleeve

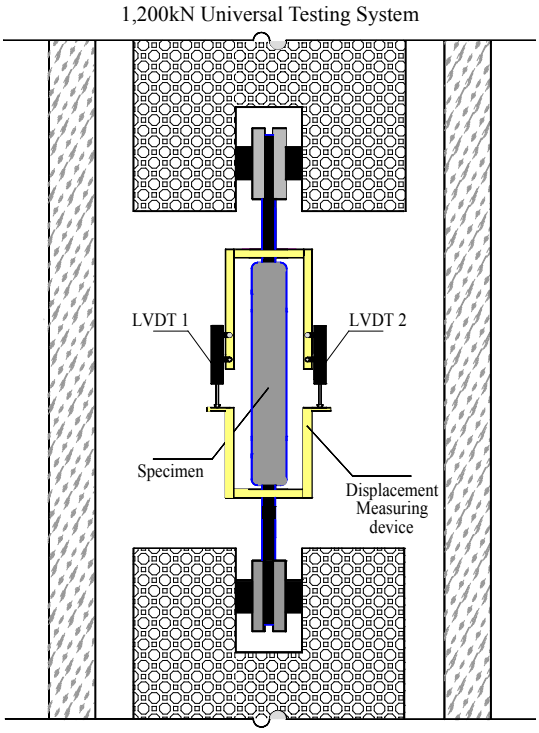

Figure 4. Specimen setup for cyclic loading

2.4 Test results

Table 6 shows test results such as the maximum stress and final failure mode of the 7 specimens, and Figure 5~8 show the final failure pattern of representative specimens 37B2HM-1, 35B2NM-1, 37B2NC-1 and 37B2HC-1. In addition, Figure 9~12 show the stress-strain relationship and the distribution of axial and tangential strain in sleeve in the 4 specimens above. In these figures, stress on the vertical axis of (a) was obtained from dividing load applied to the specimens by the nominal sectional area of the reinforcing bars, and the strain of the specimens on the horizontal axis of (a) indicates the length extended in the displacement measuring distance of the specimen expressed in percentage. Also, the vertical axes of (b) and (c) indicate, respectively, axial and tangential strain in sleeve by major loading stage, and the horizontal axes are the locations of strain gauges on sleeve surface as marked in Figure 3.

Table 6. Test results

No.	Specimens	Maximum stress (MPa)	Final failure mode*1
1	27B'1NM-1	658	R
2	37B2HM-1	668	B
3	37B2NM-1	680	B
4	35B2NM-1	556	B
5	37B2NC-1	678	R
6	37B2HC-1	698	B
7	35B2NC-1	557	B

(Note) *1 : R=Reinforcing bar fracture,
B=Bond failure (Bar slipped out of the mortar.)

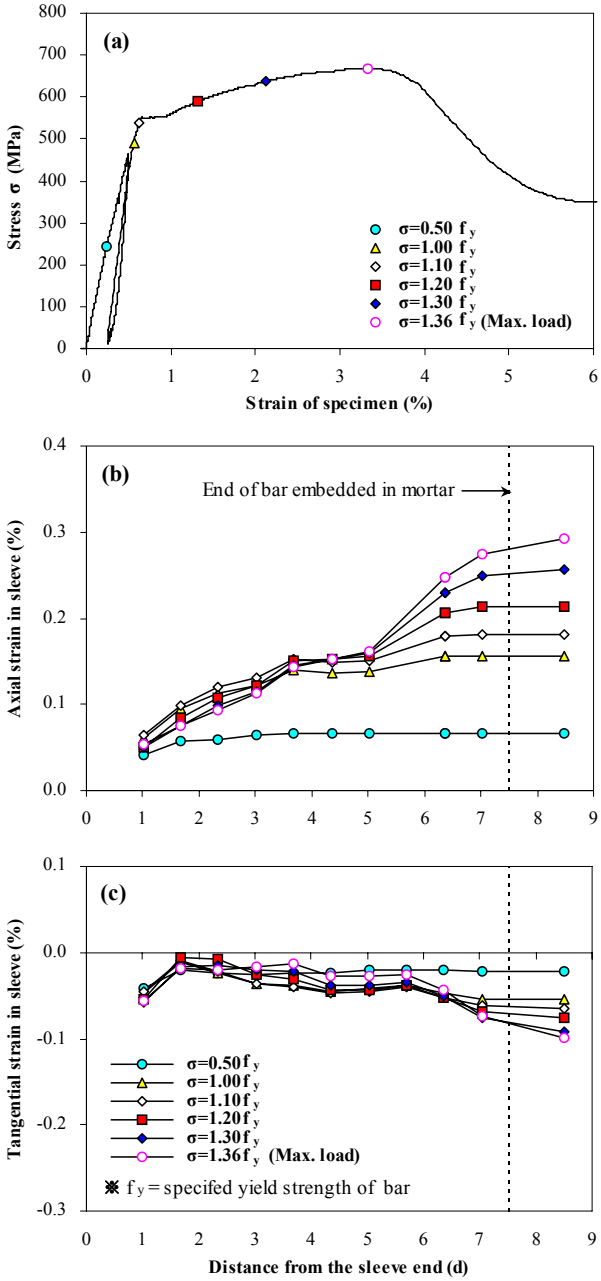

Figure 9. Stress-strain relationship and the distribution of axial and tangential strain in sleeve (37B2HM-1)

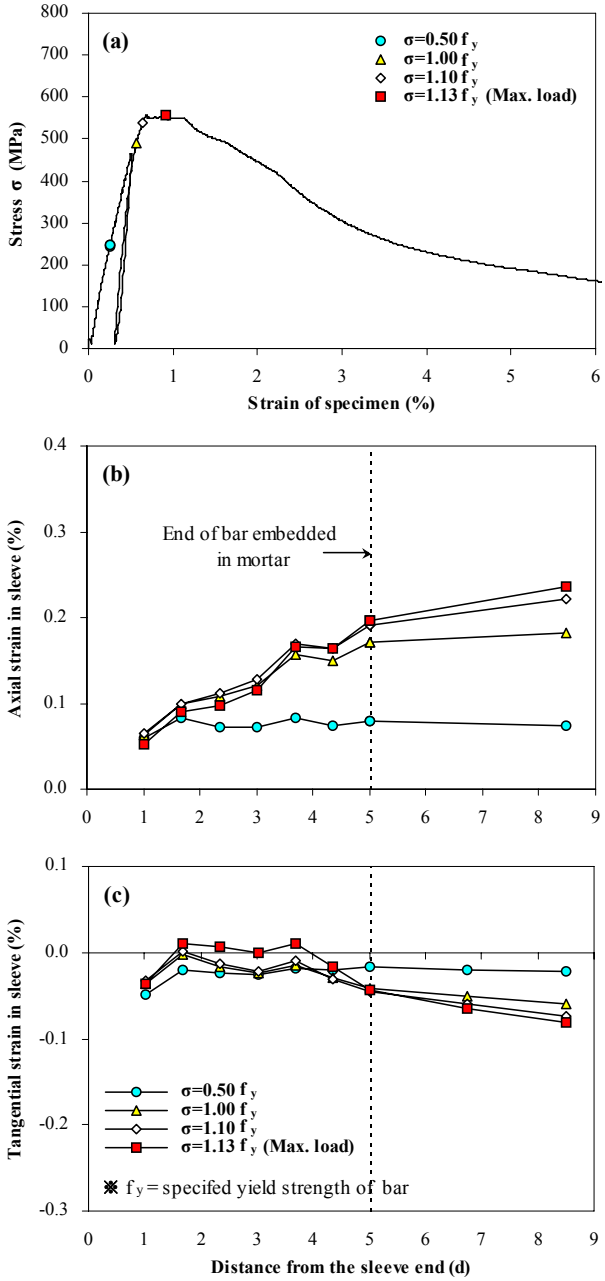

Figure10. Stress-strain relationship and the distribution of axial and tangential strain in sleeve (35B2NM-1)

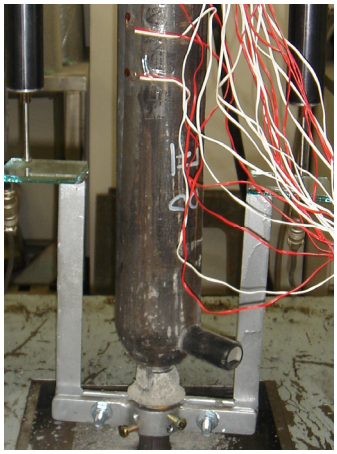

Figure 5. Final failure pattern (Specimen 37B2HM-1)

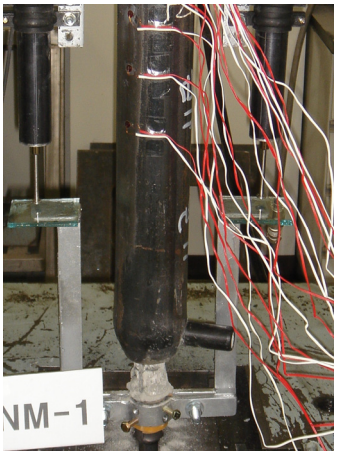

Figure 6. Final failure pattern (Specimen 35B2NM-1)

Figure 7. Final failure pattern (Specimen 37B2NC-1)

Figure 8. Final failure pattern (Specimen 37B2HC-1)

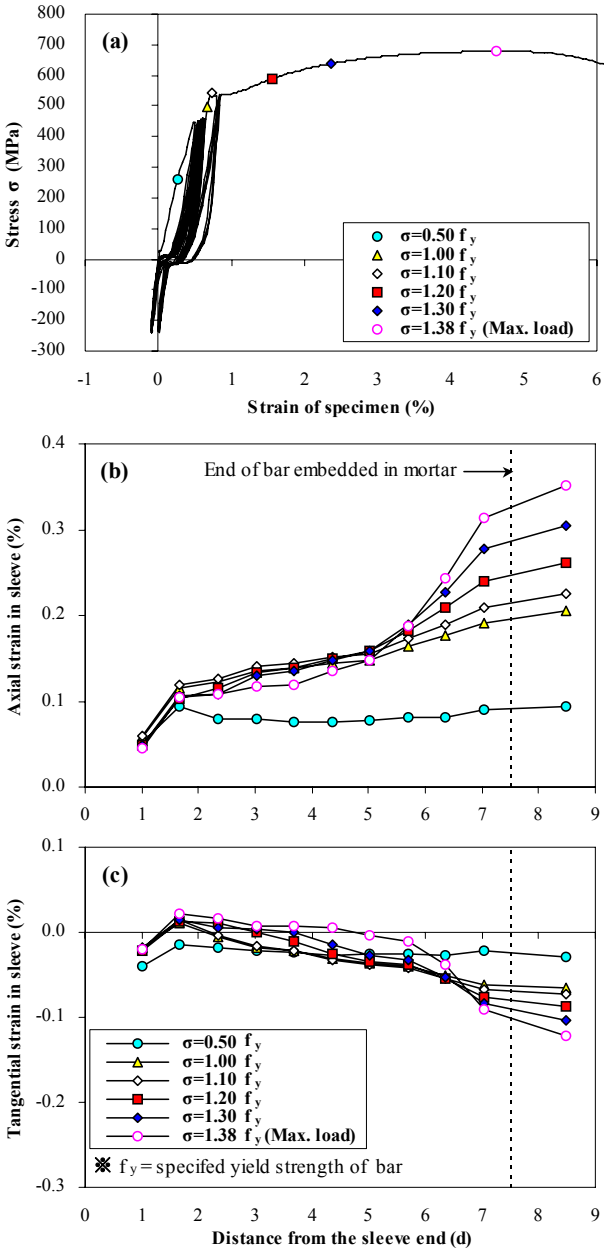

Figure 11. Stress-strain relationship and the distribution of axi`al and tangential strain in sleeve (37B2NC-1)

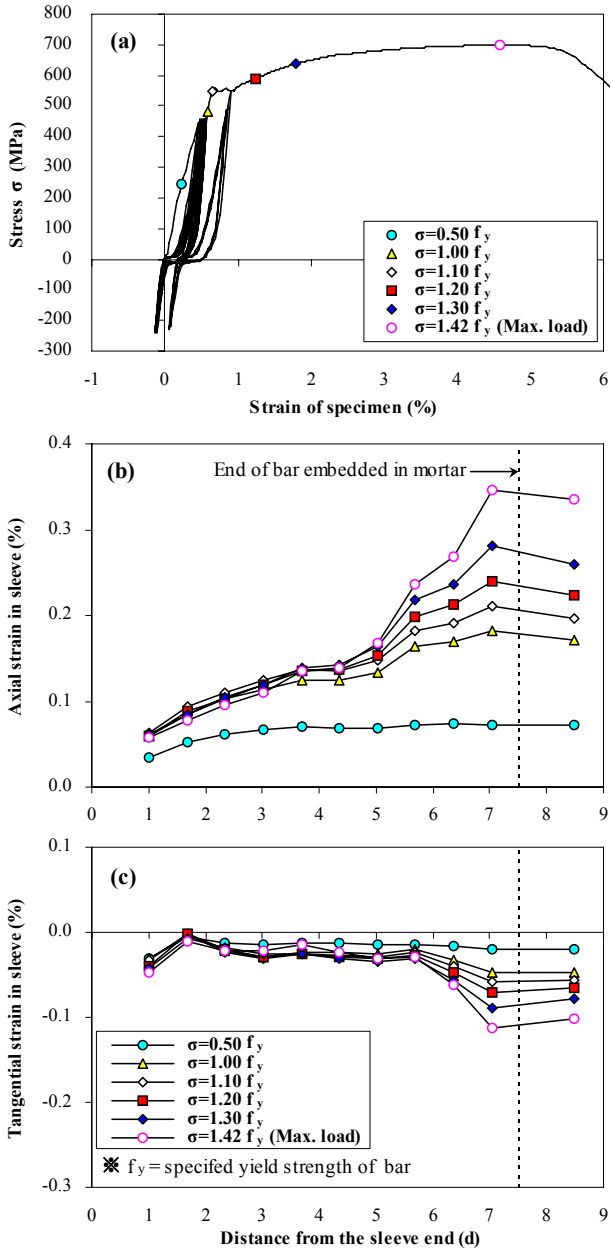

Figure 12. Stress-strain relationship and the distribution of axial and tangential strain in sleeve (37B2HC-1)

As shown in Figure 9~12, in specimens 37B2HM-1, 35B2NM-1, 37B2NC-1 and 37B2HC-1, the distribution of axial strain in sleeve was commonly low in the tension direction near the ends of the sleeve and increased as it came closer to the center of the sleeve, and this tendency was more obvious when the level of stress applied to the specimens was high. Moreover, the increase rate was higher in a position distant from the sleeve ends.

Contrary to axial strain, tangential strain in sleeve distributed mainly in the compression direction. With the increase of stress applied to the specimen, strain in the compression direction decreased in a position close to the sleeve ends and increased in a position distant from the sleeve ends. On the other hand, a large strain in the compression direction was observed in the position closest to the sleeve end (1.0d apart from the end) compared to that in other adjacent positions, showing the change of stress at the sleeve end.

Particularly in the specimens in which the development length of reinforcing bars was 7.5d, the increase rate of axial and tangential strain in sleeve was significantly high in a position over 6d apart from the sleeve end. This tendency was more remarkable in the specimen with cyclic loading (37B2HC-1) than that with monotonic loading (37B2HM-1), and more in the specimen with bond failure (37B2HC-1) than that with the bar fracture (37B2NC-1) among the specimens with cyclic loading.

What is more, when the maximum load was applied, the 4 specimens above that used D32 bars showed the largest axial and tangential strain in sleeve in the tension and compression direction in the innermost one among the positions on the sleeve where bars were embedded. Here, the axial strain in sleeve was around 0.27% in specimen 37B2HM-1 (development length of reinforcing bar 7.5d, monotonic loading, bond failure), 0.19% in 35B2NM-1 (development length of reinforcing bar 5d, monotonic loading, bond failure), 0.31% in 37B2NC-1 (development length of reinforcing bar 7.5d, cyclic loading, bar fracture) and 0.34% in 37B2HC-1 (development length of reinforcing bar 7.5d, cyclic loading, bond failure). On the other hand, the largest tangential strain was around 0.07% in 37B2HM-1, 0.04% in 35B2NM-1, 0.09% in 37B2NC-1 and 0.11% in 37B2HC-1.

3. BOND STRENGTH IN CONSIDERATION OF THE CONFINING EFFECT OF STEEL PIPE SLEEVE

3.1 Computation and analysis of the lateral confining pressure of sleeve

In mortar-filled sleeve splice, stress is transmitted to the mortar filled in the sleeve through the reinforcing bars, and the sleeve has a confining effect that suppresses splitting cracks of the filling mortar. In addition, from the equilibrium condition of force occurring between the sleeve and filling mortar in the splice, confining pressure f_n working on the sleeve can be computed as follows, which was presented in the existing research (Einea et al., 1995; Ahn et al., 2003).

$$f_n = \frac{2S_{sx}}{d_i \cdot \Delta l} = \frac{2\sigma_{sx} \cdot t \cdot \Delta l}{d_i \cdot \Delta l} = \frac{2\sigma_{sx} \cdot t}{d_i} \quad (1)$$

where, S_{sx} : Tangential force working on the small length of the sleeve
d_i : Internal diameter of the sleeve
$\Delta\ell$: Small length of the sleeve
σ_{sx} : Tangential stress working on the sleeve
t : Thickness of the sleeve

In addition, because not only tangential force but also axial force works in the sleeve above, the relationship between stress and strain can be expressed as follows.

$$\varepsilon_{sx} = \frac{\sigma_{sx}}{E_{sx}} - \frac{\sigma_{sy}}{E_{sy}}\nu_{sy} \quad (2)$$

$$\varepsilon_{sy} = \frac{\sigma_{sy}}{E_{sy}} - \frac{\sigma_{sx}}{E_{sx}}\nu_{sx} \quad (3)$$

where, ε_{sx} : Tangential strain working on the sleeve
ε_{sy} : Axial strain working on the sleeve
σ_{sx} : Tangential stress working on the sleeve
σ_{sy} : Axial stress working on the sleeve
E_{sx} : Modulus of elasticity tangential in the sleeve
E_{sy} : Modulus of elasticity axial in the sleeve
ν_{sx} : Poisson's ratio tangential in the sleeve
ν_{sy} : Poisson's ratio axial in the sleeve

Moreover, from Equation (2) and (3) above can be obtained tangential stress σ_{sx} working on the sleeve as follows.

$$\sigma_{sx} = \frac{E_{sx}}{1-\nu_{sx}\nu_{sy}}(\varepsilon_{sx} + \nu_{sy} \cdot \varepsilon_{sy}) \quad (4)$$

If Equation (4) above is inserted to Equation (1), confining pressure f_n working on the sleeve is as follows.

$$f_n = \frac{2E_{sx}}{1-\nu_{sx}\nu_{sy}}(\varepsilon_{sx} + \nu_{sy} \cdot \varepsilon_{sy})\frac{t}{d_i} \quad (5)$$

Using Equation (5) above, we computed the confining pressure of sleeve in 4 representative specimens by major loading stage, and presented the results in Figure 13. In addition, Figure 14 compared confining pressure by sleeve under the maximum load in 6 representative specimens. Here, tangential and axial strain working on the sleeve was computed using data obtained from the two-direction strain gauges attached to the specimens, and the sleeve's modulus of elasticity (E_{sx}) was obtained from the test results of the materials. And Poisson's ratio of the sleeve (ν_s) was set to 0.3.

As in Figure 13 (a) and (b), for specimens in which monotonic loading was performed and bond failure occurred finally, from the low load stage, confining pressure was higher in all the positions of sleeve, in which bars

were embedded, except the position 1.0d apart from the sleeve end when the development length of reinforcing bar was 5d (35B2NM-1) than when it was 7.5d (37B2HM-1), and with the increase of load, confining pressure increased at a nearly constant rate in all the positions of sleeve in which bars were embedded in mortar.

For the specimens in which the development length of bar was 7.5d and bond failure occurred finally (37B2HM-1, 37B2HC-1), as in Figure 13 (a) and (d), regardless of loading method, the confining pressure of the sleeve at a relatively low load stage was relatively high in a position near the sleeve end, except the position 1.0d apart from the sleeve end and decreased as it came closer to the center of the sleeve, but with the increase of load, confining pressure on the center of the sleeve became relatively higher than that on the sleeve end.

As in Figure 13 (c) and (d), between the specimens in which the development length of bar was 7.5d and cyclic

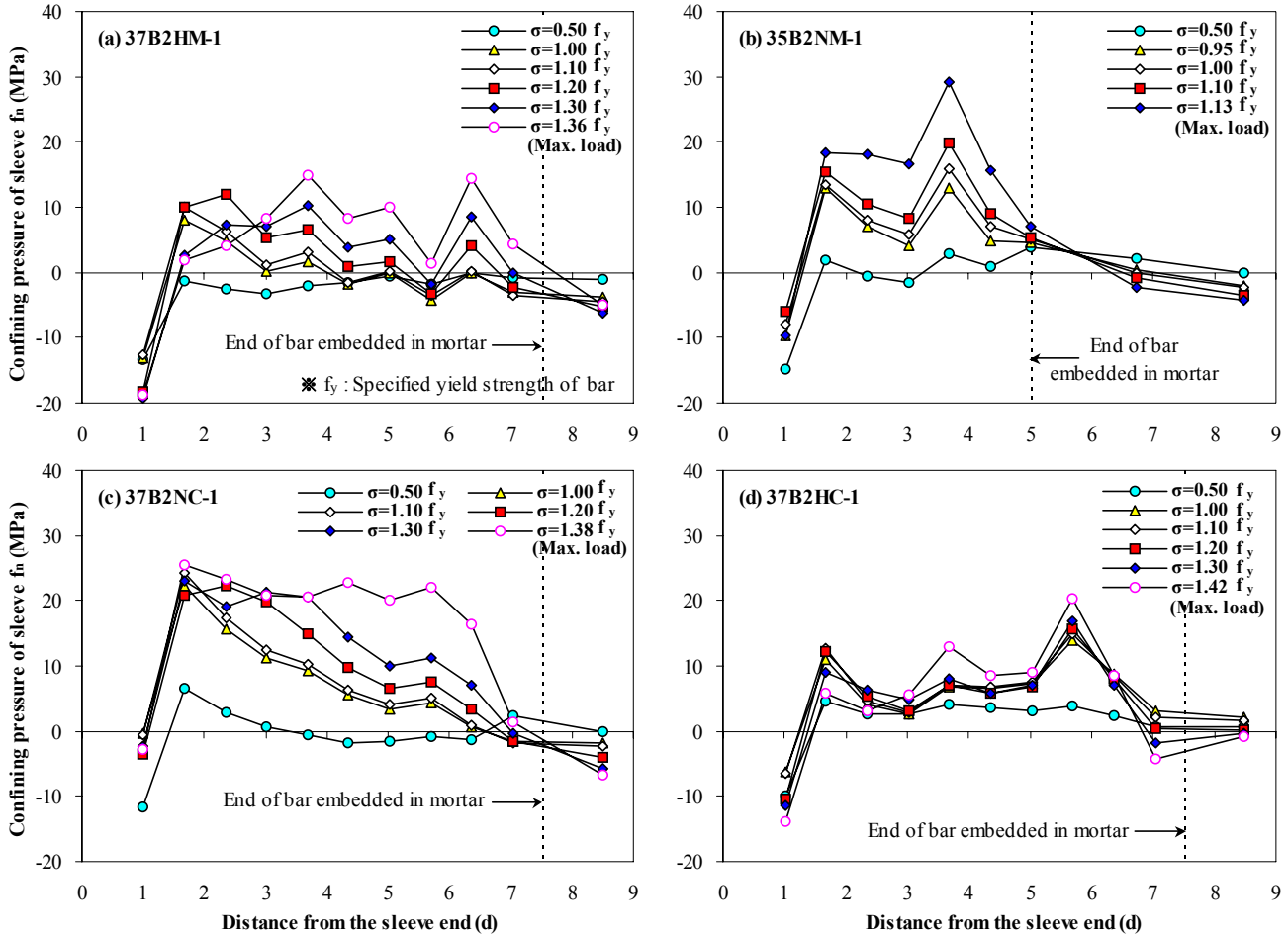

Figure 13. Distribution of confining pressure by sleeve according to loading stage in representative specimens

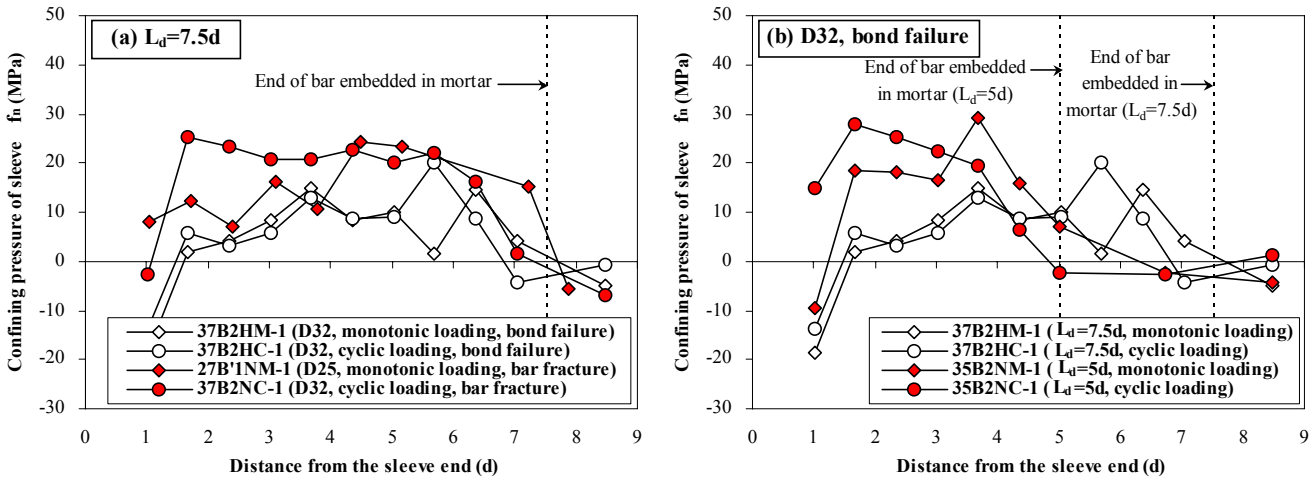

Figure 14. Comparison of confining pressure of sleeve at the maximum load in representative specimens

loading was performed (37B2NC-1, 37B2HC-1), specimen 37B2NC-1 that had bar fracture showed different distribution of sleeve confining pressure from specimen 37B2HC-1 that had final bond failure. That is, despite the increase of load, the specimen with reinforcement fracture (37B2NC-1) maintained constant confining pressure of sleeve in a position near the sleeve end, and with the increase of load, confining pressure increased in a position near the center of the sleeve and the distribution of confining pressure became almost even in all the positions of sleeves in which bars were embedded in mortar when the load reached its highest level.

As in Figure 14 (a) and (b), when the maximum load was applied, specimens (37B2HM-1 and 37B2HC-1, 35B2NM-1 and 35B2NC-1), which were under the same conditions except loading method, showed little difference in confining pressure of sleeve according to loading method, and specimens 27B'1NM-1 and 37B2NC-1, which were under the same conditions except the bar size and loading method, also showed relatively similar distribution of confining pressure.

In Figure 14 (a), however, different from the specimens with bond failure, the specimens with bar fracture showed almost even distribution of relatively high confining pressure in all the positions of sleeves in which bars were embedded in mortar. In addition, as in Figure 14 (b), different from specimens (37B2HM-1, 37B2HC-1) that had a long development length of reinforcing bar when the maximum load was applied, those (35B2NM-1, 35B2NC-1) that had a short development length of reinforcing bar showed high confining pressure in the most positions of sleeves in which bars were embedded in mortar.

In addition, when the maximum load was applied, the highest confining pressure of sleeve was 15~20MPa in specimens in which the development length of reinforcing bar was 7.5d and there was final bond failure, 24~25MPa in specimens in which bars fractured finally, and 28~29MPa in specimens in which the development length of reinforcement was 5d and there was final bond failure.

3.2 Computation of bond strength by Untrauer and Henry's Eqution

Untrauer and Henry (1965) proposed bond strength in consideration of the lateral confining effect as follows.

$$U = \left(18 + 0.45\sqrt{f_n}\right)\sqrt{f'_c} \qquad (6)$$

where, U : Bond strength [psi]
f_n : Lateral confining pressure [psi]
f'_c : Concrete compressive strength [psi]

If Equation (6) above is converted to the unit of SI and is applied to mortar-filled sleeve splice on which lateral confining pressure works by sleeve, bond stress can be expressed as follows.

$$\tau = \left(1.49 + 0.45\sqrt{f_n}\right)\sqrt{f_m} \qquad (7)$$

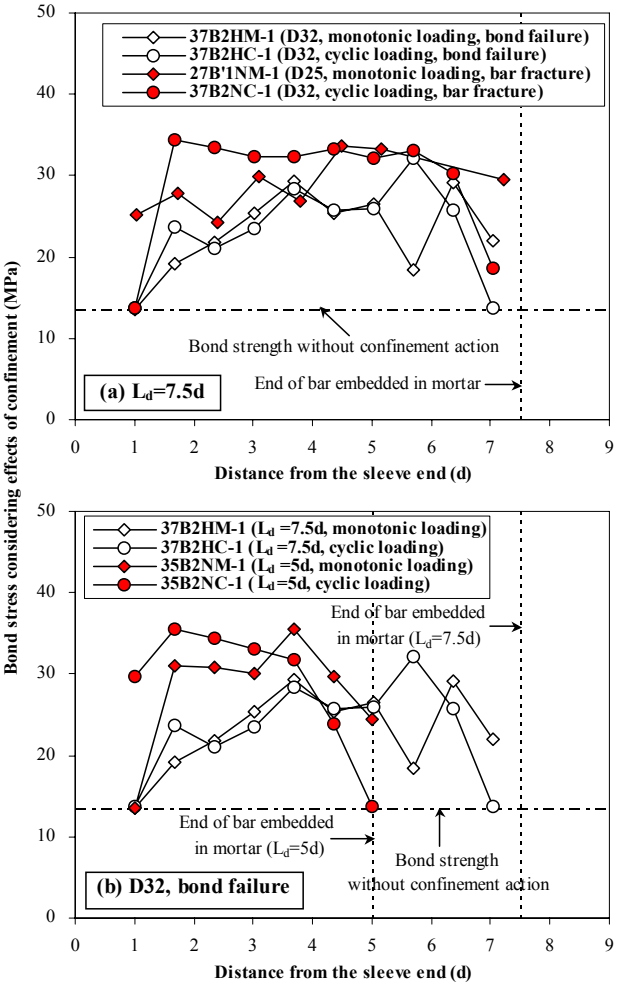

Figure 15. Comparison of bond stress in consideration of confining pressure at the maximum load in representative specimens

where,
τ : Bond stress of mortar-filled sleeve splice [MPa]
f_n : Lateral confining pressure by sleeve [MPa]
f_m : Compressive strength of filling mortar [MPa]

Figure 15 shows bond stress within the range of the development length of reinforcing bar computed by applying lateral confining pressure at the maximum load obtained for the 6 representative specimens of this test to Equation (7) above. In Figure 15, bond stress was up to 2.1~2.6 times higher than that in case there was no confinement

Table 7. Comparison between the measured maximum strength and computed bond strength in specimens with bond failure

Specimens	Measured result P_{test} (kN)	Computed value $P_{b.com}$ (kN)	$P_{test} / P_{b.com}$
37B2HM-1	530.2	530.5	0.999
37B2NM-1	539.9	488.0	1.106
35B2NM-1	441.8	416.1	1.062
37B2HC-1	554.9	532.1	1.043
35B2NC-1	442.4	442.6	1.000
Mean			1.042
Coefficient of variation			0.043

Table 8. Comparison between the measured maximum strength and computed bond strength in specimens with bar fracture

Specimens	Measured result P_{test} (kN)	Computed value $P_{b.com}$ (kN)	P_{test} / $P_{b.com}$
27B'1NM-1	333.5	424.8	0.785
37B2NC-1	538.7	662.6	0.813
Mean			0.799

action resulting from the lateral confining effect by sleeve. In addition, Table 7 and 8 show a comparison of the computed ultimate bond strength and the measured maximum strength for 5 specimens with bond failure and 2 specimens with the bar fracture, respectively. Here, the computed bond strength ($P_{b.com}$) of each specimen was obtained from the equation below.

$$p_{b.com} = \int_0^{L_d} (\tau \cdot \pi d_b) dx \quad (8)$$

where,

L_d : The development length of reinforcing bar embedded in sleeve [mm]

τ : The bond stress of mortar-filled sleeve splice computed by Equation (7) [MPa]

d_b : The nominal diameter of embedded bars [mm]

dx : Small part of the development length of embedded bars [mm]

The computation of bond strength for each specimen above assumed that there is no lateral confining pressure on the sleeve end without a strain gauge attached in the test.

As in Table 7, the bond strength computation method proposed by Untrauer and Henry, which considers the lateral confinement effect, estimated the measured maximum strength of the 5 specimens with final bond failure within an error rate of 5% on the average, and the coefficient of variation among the specimens was around 4.3%. On the other hand, when the bond strength computation equation was applied to the 2 specimens with the bar fracture, as in Table 8, the strength was around 20% higher than the measured maximum strength of the specimens. It is presumed that final bond failure did not occur in the two specimens and instead the reinforcing bars fractured because the bond strength of the specimens was relatively higher than the fracture strength of the bars as shown in the results of computation above.

4. CONCLUSIONS

In order to examine the effect of confinement in mortar-filled steel pipe sleeve splice, we prepared actual-size specimens of steel pipe sleeve splice for reinforcing bar D32 and D25 with strain gauges attached on the sleeve surface, and conducted a loading. From the test results were drawn conclusions as follows on how the confining effect of steel pipe sleeve affects the bond strength of mortar-filled steel pipe sleeve splice.

1) When confining pressure working on splice of reinforcement was computed from the distribution of strain on sleeve surface measured in the test, confining pressure of up to 15~29MPa worked on the specimens, and the confining pressure showed the tendency of increasing with the decrease of the development length of reinforcing bar and was higher in specimens with the bar fracture than those with bond failure.

2) When confining pressure obtained from strain measured on sleeve surface was applied to the bond strength computation equation proposed by Untrauer and Henry, which considers the lateral confinement effect, the lateral confining effect by sleeve increased bond stress up to 2.1~2.6 times higher.

3) The bond strength computation method proposed by Untrauer and Henry estimated the test results within an error rate of 5% on the average.

REFERENCES

Ahn, B. I., Kim, H. K., and Park, B. M. (2003) "Confining Effect of Mortar Grouted Splice Sleeve on Reinforcing Bar," Journal of the Korea Concrete Institute, V.15, No.1: 102-109

Architectural Institute of Japan. (1986) "Recommendation for Detailing and Placing of Concrete Reinforcement," 271-279

Ase, M. et al. (1996) "Study for Practical Application of Grout Filled Connectors for High Strength Reinforcing Bars(No. 1 Performance of the grout filled connector with SD490 reinforcing bars)," Summaries of Technical Papers of Annual Meeting Architectural Institute of Japan, C-2, Structures Ⅳ: 743-744

ASTM C 109/C 109M. (1995) "Standard Test Method for Compressive Strength of Hydraulic Cement Mortars (Using 2-in. or [50-mm] Cube Specimens)," 385-389

Einea, A., Yamane, T., and Tadros, M. K. (1995) "Grout-Filled Pipe Splices for Precast Concrete Construction," PCI Journal, January-February: 82-93

Kim, H. K. (1998) "Development of Grout-Filled Splice Sleeve System and Estimation of its Mechanical Performance under Monotonic Loading," Journal of Architectural Institute of Korea, V.14, No.8: 63-73

Kim, H. K. (2008) "Structural Performance of Steel Pipe Splice for SD500 High-strength Reinforcing Bar under Cyclic Loading," Architectural Research, Vol.10, No.1: 13-23

Lee, L. H., Yi, W. H., Kim, B. K., Lee, Y. J., and Lee, D. W. (1997) "Experimental Study on Reinforced-Bar Connection with Steel Pipe Sleeve," Journal of Architectural Institute of Korea, V.13, No.3: 241-250

Lee, S. H., and Kim, H. K. (2007) "Development of Steel Pipe Splice Sleeve for High Strength Reinforcing Bar(SD500) and Estimation of its Structural Performance under Monotonic Loading," Journal of the Korea Institute for Structural Maintenance Inspection, V.11, No.6: 169-180

Untrauer, R. E., and Henry, R. L. (1965) "Influence of Normal Pressure on Bond Strength," ACI Journal, May: 577-585

(Data of Submission : 2008. 5. 13)